Radial and orientational solvation structure of the sodium chloride ion pair in dimethyl sulfoxide

Ashok K. Das and B. L. Tembe

Citation: J. Chem. Phys. **108**, 2930 (1998); doi: 10.1063/1.475680
View online: http://dx.doi.org/10.1063/1.475680
View Table of Contents: http://jcp.aip.org/resource/1/JCPSA6/v108/i7
Published by the American Institute of Physics.

Radial and orientational solvation structure of the sodium chloride ion pair in dimethyl sulfoxide

Ashok K. Das and B. L. Tembe
Department of Chemistry, Indian Institute of Technology, Bombay, Powai, Mumbai, 400 076, India

(Received 28 July 1997; accepted 5 November 1997)

The structures of the solvation shells around each ion of the Na^+–Cl^- ion pair in liquid dimethyl sulfoxide (DMSO) have been studied in terms of the ion–solvent radial distribution functions (RDFs) and the ion–solvent orientational distribution functions (ODFs) at the three interionic separations of 2.6 Å, 4.9 Å, and 7.2 Å. The solvation shell around the sodium ion consists of only three DMSO molecules at the ion–ion separation of 2.6 Å and this number grows to five DMSO molecules at interionic separation 4.9 Å and beyond. These are in contrast with the octahedral solvation shells around sodium ion in water at all ion–ion separations, where the chloride ion replaces a molecule of water only at a short interionic distance of 2.7 Å. The orientational structure of the solvent around the ion pair has been probed by dividing the DMSO solvent into five spatial regions and analyzing the angular distributions in each region. In the shell near the Na^+ ion, the orientation of the sulphur–oxygen vector in DMSO is sharply peaked about 155° away from the sodium–sulphur vector for all the three interionic distances. Similarly, the orientation of the DMSO dipole vector is also sharply peaked about 155° away from the sodium–DMSO center of mass (COM) vector. In the shell near the Cl^- ion, the orientation of the sulphur–oxygen vector with respect to the chloride-sulphur vector shows broader peaks in the range 20°–100°. The solvent dipole vector gets oriented in a similar fashion with respect to the chloride–COM vector in this shell. In the regions far from the Na^+ and Cl^- solvation shells, both the sulphur–oxygen vector and the solvent dipole vector have broad distributions covering all the angles except the parallel and the antiparallel alignments. The angles between the Na^+–S–O plane (or the Cl^-–S–O plane) and the S–Na^+–Cl^- plane do not show a preference for any specific inclination, in any of the spatial regions around the ion pair. These broad distributions are indicative of a weaker second shell around the ion pair in DMSO than the second shell found in water and are a consequence of the near absence of hydrogen bonding in DMSO. © *1998 American Institute of Physics.* [S0021-9606(98)52206-4]

I. INTRODUCTION

Relative orientations and alignments of the reactants during reactive collisions and the spatial arrangements of the solvent molecules around the reacting species contribute significantly to the macroscopic reaction rates in solution media.[1,2] In the much studied ion pair interconversion process,[3–8] a contact ion pair (CIP) configuration crosses over to a solvent separated ion pair (SSIP) configuration and vice versa. These two states are usually separated by a free energy barrier of several k_BT (k_B is the Boltzmann constant and T is the absolute temperature). The role of the solvent in influencing such processes has been studied in detail by many authors.[7–11] These studies involve the following steps: (1) calculation of the ion–ion potential of mean force (PMF), $W(r)$ in the presence of the solvent, (2) calculation of the stochastic forces, $R(t)$ exerted by the solvent molecules on the reactants, (3) computation of the solvent friction kernels, $\xi(t)$ and, (4) evaluation of the transmission coefficient, κ employing either the Kramers' theory[12] (κ_{Kr}) or the Grote–Hynes' theory[13] (κ_{GH}) through the friction coefficient, ξ. An alternative approach[7] to this is to perform molecular dynamics (MD) simulation on an ensemble containing the reactant ions in presence of an adequate number of solvent molecules in a simulation box with suitable boundary conditions to represent the bulk of the solvent. In this technique, the reactive trajectories are followed from the transition state (TS) for a sufficiently long time. The crossing-recrossing occurrences across the barrier top of the PMF are used to estimate the magnitude of the transmission coefficient (κ_{MD}). The computed value of the transmission coefficient κ measures the deviation of the rate constant from the ideal transition state theory (TST) value,[7]

$$k_{rate} = \kappa \cdot k_{TST}, \tag{1}$$

where k_{TST} is the TST rate constant. Equilibrium solvation structures around each reactant will influence the magnitude of κ. Although the exact quantitative relations regarding the solvolytic effects are not fully established,[14] the departure of κ from its ideal value of unity can be explained as follows. The reacting system may reside either in the nonadiabatic regime or in the polarization caging regime.[15] In the nonadiabatic regime, the solvent molecules cannot move significantly during the passage of the reacting ion pair across the PMF barrier. The polarization caging regime is characterized by strong solvent forces.[15] In this regime, considerable rearrangement of the solvent cage takes place during the transformation of the reactant state into the product state across the barrier top. Microscopically, this can be studied by ana-

lyzing the solvation shells around the participating ions continuously during the motion along the reaction coordinate. This would entail a knowledge of the spatial distribution of the solvent molecules around each reactant ion. The radial distributions of the solvent molecules around the ions do not contain adequate structural informations that are required and must be supplemented by the orientational distributions of the solvent molecules. The importance of the orientational distributions in probing the solvation structure of the Na^+-Cl^- ion pair in water has been emphasized by Belch *et al.*[16]

Apart from the use of the ODFs as the tools to probe the solvation shells around the reacting ions, a knowledge of the orientational distributions in pure solvents has also been exploited to calculate the contribution to entropy in liquid water by Lazaridis and Karplus.[17] Orientational distributions of the various vectors of large molecules such as phospholipids at the water–hydrocarbon bilayers using all-atom MD simulations have reproduced many experimental observables.[18] These studies are also useful in studying the diffusion of small molecules and their effects on lipid structure and dynamics.[19] While detection of the CIPs and SSIPs for large ionic systems such as 1-alkyl-4-cyanopyridinium iodide has been possible in a large number of solvents[20,21] through estimation of the intrinsic molar intensities of charge transfer bands and conductance measurements, the orientational contributions of the solvent molecules has not been probed experimentally so far.

The extensive MD simulations and quantum mechanical analysis of the effect of dimethyl sulfoxide (DMSO) on enzyme structure and dynamics reported by Zheng and Ornstein[22] have established that the solvent DMSO is capable of stripping water molecules as well as metal ions away from the protein surface through a ''soaking'' mechanism. The solvent DMSO has been becoming increasingly important due to its cryoprotectant properties for membranes and proteins,[23] ability to solvate biomolecules, antiviral and antibacterial activity and antiinflammation effect.[24] Microscopic details of these ion–DMSO interactions will further assist in understanding the rate enhancements caused when small quantities of salts are added to DMSO during synthesis.[25]

We have reported the ion–ion PMF[26,27] as well as the transmission coefficients[11] for the Na^+-Cl^- ion pair in dimethyl sulfoxide (DMSO) in our earlier papers. In the present article, we present the detailed analysis of the radial and orientational distributions of the solvent molecules around the ion pair in DMSO as a function of ion–ion distance. The following section describes briefly the MD simulation method and the computation of the ion-solvent radial and orientational distribution functions. The results and discussion on RDFs and ODFs are presented in Sec. III and IV, respectively. The conclusions are summarized in the last section.

II. THE MD SIMULATION METHOD

The choice of the ion–solvent and solvent–solvent potentials and the system for performing the MD simulations have been discussed in detail in our earlier papers.[11,26,27] We recount here only the relevant informations for the present work. We have considered 125 DMSO molecules, one Na^+ ion and one Cl^- ion residing in a cubical simulation box of edge length 24.506 Å. The site–site interaction potentials are of (12-6-1) form consisting of Lennard-Jones and Coulombic contributions. The non-Coulombic part has been calculated using a cutoff of radius equal to half of the box length. The long range Coulombic part is computed using the reaction field method.[28] Conventional periodic boundary conditions were used and the equations of motion were integrated with a time step of 0.005 ps using the Verlet algorithm.[29] Intramolecular lengths and geometries were constrained using the SHAKE algorithm.[30] In each MD run, the interionic separation was also constrained at the selected distances of 2.6 Å, 4.9 Å, and 7.2 Å. A temperature of 298 K was maintained during all the simulation runs. Equilibrated solvent configurations have been generated for each of the ion–ion distances reported. These distances are the same which have been identified as the CIP (2.6 Å), the TS (4.9 Å), and the SSIP (7.2 Å) for the Na^+-Cl^- ion pair in DMSO.[11] For each of these distances the system was equilibrated for 10–20 ps followed by a production period of 50 ps. The radial and orientational distributions are collected at each time step and averaged over the entire simulation. The ion–solvent radial distribution functions are computed for (Na^+-O), (Na^+-S), (Na^+-CH_3), (Cl^--O), (Cl^--S), and (Cl^--CH_3) pairs. The orientational distribution functions are computed in terms of two functions, viz. $[P(\theta_i)]$ and $[P(\phi_i)]$. The angles (θ_i) are the inverse cosines of the dot products of the ion–sulphur and sulphur–oxygen bond vectors (the bond vectors are denoted by the superscript line joining one atom/ion to another ion/atom),

$$\theta_1 = \cos^{-1}[(\overline{Na^+-S})\cdot(\overline{S-O})], \tag{2a}$$

$$\theta_2 = \cos^{-1}[(\overline{Cl^--S})\cdot(\overline{S-O})]. \tag{2b}$$

The angles (ϕ_i) are defined through the scalar products of pairs of unit vectors $(\hat{u}_i)$ which in turn are the cross products of ion–ion, ion–solvent atom and solvent bond vectors. The unit vectors $(\hat{u}_i)$ are

$$\hat{u}_1 = (\overline{Na^+-S})\times(\overline{S-O}), \tag{3a}$$

$$\hat{u}_2 = (\overline{Na^+-S})\times(\overline{Na^+-Cl^-}), \tag{3b}$$

$$\hat{u}_3 = (\overline{Na^+-S})\times(\overline{S-CH_3^{mid}}), \tag{3c}$$

$$\hat{u}_4 = (\overline{Cl^--S})\times(\overline{S-O}), \tag{3d}$$

$$\hat{u}_5 = (\overline{Cl^--S})\times(\overline{Cl^--Na^+}), \tag{3e}$$

$$\hat{u}_6 = (\overline{Cl^--S})\times(\overline{S-CH_3^{mid}}), \tag{3f}$$

where CH_3^{mid} is the midpoint of the line joining the two CH_3 groups in DMSO. The angles (ϕ_i) are

$$\phi_1 = \cos^{-1}(\hat{u}_1\cdot\hat{u}_2), \tag{4a}$$

$$\phi_2 = \cos^{-1}(\hat{u}_2\cdot\hat{u}_3), \tag{4b}$$

$$\phi_3 = \cos^{-1}(\hat{u}_1\cdot\hat{u}_3), \tag{4c}$$

$$\phi_4 = \cos^{-1}(\hat{u}_4\cdot\hat{u}_5), \tag{4d}$$

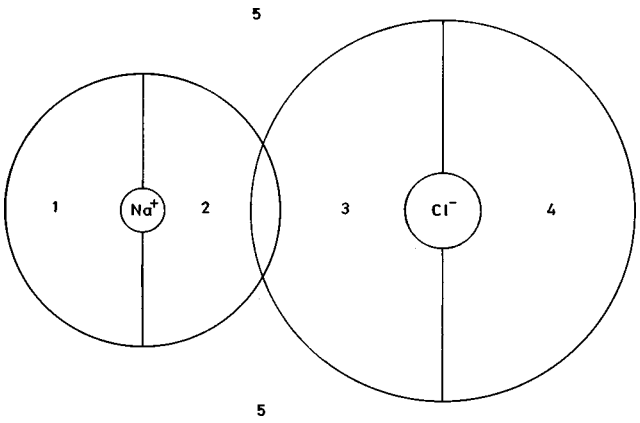

FIG. 1. The five spatial regions around the Na^+Cl^- ion pair in DMSO.

$$\phi_5 = \cos^{-1}(\hat{u}_5 \cdot \hat{u}_6), \tag{4e}$$

$$\phi_6 = \cos^{-1}(\hat{u}_4 \cdot \hat{u}_6). \tag{4f}$$

The angles ϕ_1, ϕ_2, ϕ_4, and ϕ_5 give the magnitudes of the angles between two planes one of which is the plane containing the Na^+ ion, the Cl^- ion and the S atom. For example, the angle ϕ_1 gives the orientation of the plane containing the Na^+ ion, the S atom and the O atom with respect to the plane containing the Na^+ ion, the Cl^- ion and the S atom. Similarly, the angle ϕ_5 gives the orientation of the plane containing the Cl^- ion, the S atom, and the CH_3^{mid} with respect to the plane containing the Na^+ ion, the Cl^- ion and the S atom. The angles ϕ_3 and ϕ_6 give the relative orientations of the planes within the molecule with respect to the ion–sulphur axis (Na^+–S and Cl^-–S, respectively) and provide only the intramolecular solvent orientations. We have chosen these representations for the orientations of the DMSO molecules in place of the much more detailed information that the Euler angles on each molecule can provide.

For the sake of convenience, we have divided the space in the vicinity of the ions into five distinct regions. The (θ_i) and (ϕ_i) angles are calculated in these five regions of space around the reactant ion pair. Region 1 is the hemisphere to the left of the Na^+ ion with a radius of 4.5 Å, region 2 is the hemisphere of equal radius to the right of the Na^+ ion, region 3 is the hemisphere to the left of the Cl^- ion with a radius of 6.5 Å, region 4 is the hemisphere to the right of the Cl^- ion of radius 6.5 Å and region 5 is the rest (or the bulk) of the solvent medium. These regions are shown in Fig. 1. The radii of the hemispheres are based on the first minimum in the ion–sulphur radial distribution functions. In the spatial region 1, the orientations of the DMSO molecules are measured in terms of the angles θ_1, ϕ_1, and ϕ_2. In region 4, the spatial dispositions of the DMSO molecules are described by the angles θ_2, ϕ_4, and ϕ_5. The regions 2 and 3 are sandwiched between the Na^+ and Cl^- ions; region 2 is the second half of the sphere around Na^+ while region 3 is the complementary hemisphere of region 4. The angles θ_1, ϕ_1, and ϕ_2 also describe the orientations of the solvent molecules in region 2 and the angles θ_2, ϕ_4, and ϕ_5 characterize the solvent orientations in region 3.

In each of these spatial regions the functions $P(\theta_i)$ and $P(\phi_i)$ have been calculated as

$$P(\theta_i) = \frac{N_{\theta_i}}{N} \quad i = 1,2, \tag{5a}$$

$$P(\phi_i) = \frac{N_{\phi_i}}{N} \quad i = 1,2,...,6, \tag{5b}$$

where, N_{θ_i} is the number of solvent molecules with angle θ_i in the range θ_i and $\theta_i + d\theta_i$, N_{ϕ_i} is the number of solvent molecules with angle ϕ_i in the range ϕ_i and $\phi_i + d\phi_i$ and N is the total number of molecules in that spatial region. The increments $d\theta_i$ and $d\phi_i$ were taken to be 1° each.

An analysis such as the one involving θ_i and ϕ_i can also be performed using the molecular dipole of DMSO. This is done by replacing the (ion–S) vector in Eqs. (2) and (3) with (ion–COM) vector and the (S–O) vector with (COM–DIP) vector and rewriting these equations with S replaced by the COM (COM is the center of mass of a DMSO molecule) and O replaced by the DIP (DIP is the tip of the molecular dipole). The corresponding angles can then be called as $\{\theta_i'\}$ and $\{\phi_i'\}$ and the distribution functions are referred to as $P(\theta_i')$ and $P(\phi_i')$, respectively. Since the distribution functions $[P(\theta_i')]$ do not differ very much from those of $[P(\theta_i)]$, we have presented mainly the plots for $[P(\theta_i)]$. The differences between the $[P(\phi_i')]$ and the $[P(\phi_i)]$ are neglible. We have shown only those sets of $[P(\phi_i)]$ which change significantly with interionic separation.

III. THE RADIAL DISTRIBUTION FUNCTIONS

The solvation structure of the DMSO molecules around the Na^+–Cl^- ion pair is a function of the relative positions of the solvent molecules with respect to both the ions. The description of the structure of this liquid system is usually given by the set of ion–solvent and solvent–solvent radial distribution functions (RDFs). The arrangements of the DMSO molecules around the ions are expressed in terms of the ion–solvent RDFs between the ions and the four sites of the solvent,[31]

$$g_{i\alpha}(r) = \frac{V}{N_\alpha} \cdot \frac{N_\alpha(r)}{4\pi r^2 \Delta r}, \tag{6}$$

where N_α is the number of the αth solvent site in volume V of the simulation shell and $N_\alpha(r)$ is the number of such sites in the spherical shell $(r, r+\Delta r)$ at distance r from the ion i. The RDFs have been computed for both the ions at the ion–ion distances of 2.6 Å, 4.9 Å, and 7.2 Å and are displayed in Figs. 2 and 3 for the Na^+ ion and Cl^- ion, respectively. The stronger peak intensities in the case of (Na^+–O) and (Na^+–S) pairs are clear indications of the formation of a tightly bound coordination shell around the Na^+ ion at each of the interionic separations. For the (Na^+–CH_3) pair, the intensity is much less, as the CH_3 groups are further away from the Na^+ ion. This is because the DMSO molecules are strongly oriented towards this ion with the negatively charged oxygen atoms staying within 2.1 Å from the ion. Also, the positive charge ($+0.160e$) on the two CH_3 groups and their bulkiness prevent them from coming closer to the positive Na^+ ion. In the case of (Cl^-–O) RDF, the position of the peak maximum changes with the change in the interi-

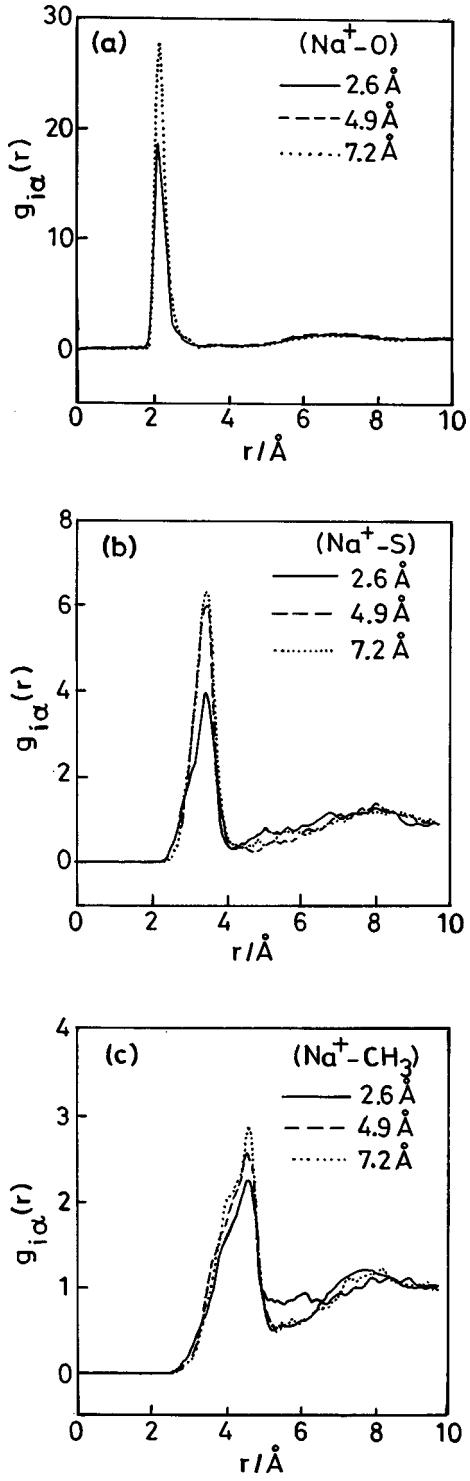

FIG. 2. The radial distribution functions for the (a) Na^+–O; (b) Na^+–S; and (c) Na^+–CH_3 pairs at the three interionic separations of 2.6 Å, 4.9 Å, and 7.2 Å.

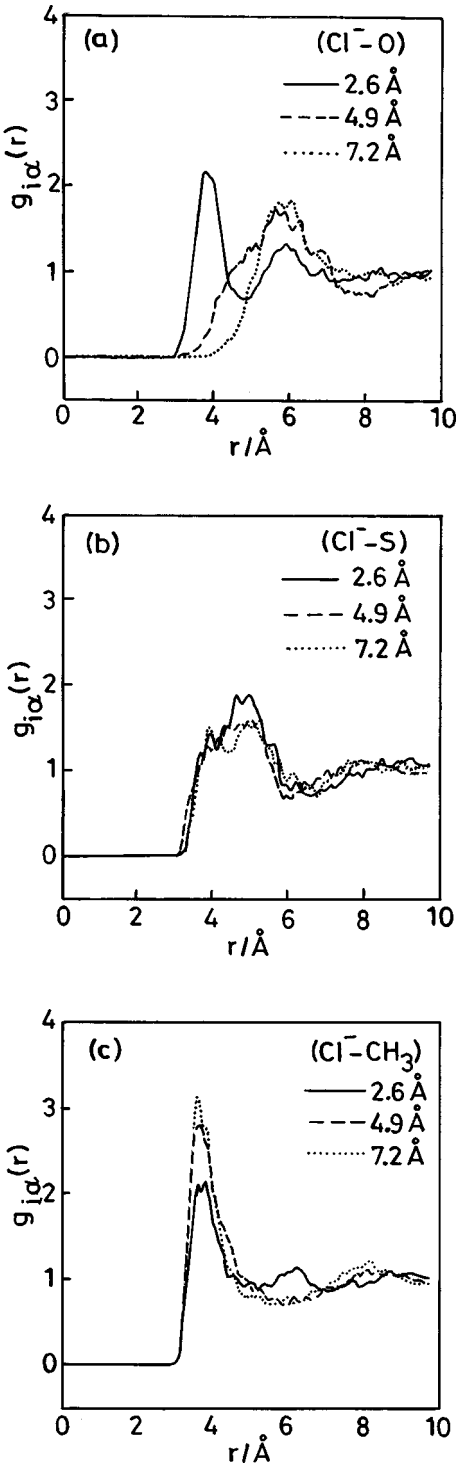

FIG. 3. The radial distribution functions for the (a) Cl^-–O; (b) Cl^-–S; and (c) Cl^-–CH_3 pairs at the three interionic separations of 2.6 Å, 4.9 Å, and 7.2 Å.

onic separation. At $r_{Na-Cl}=2.6$ Å, the oxygen atoms of DMSO closer to the Na^+ ion also contribute to the formation of the coordination shell around the Cl^- ion causing the peak maximum to appear at 3.6 Å. For $r_{Na-Cl}=4.9$ Å and 7.2 Å, the position of the (Cl^-–O) RDF peak maximum shifts to 5.9 Å. The (Cl^-–S) RDFs for the three ion–ion distances show broad first peaks between 4.3 Å and 5.8 Å, while the (Cl^-–CH_3) RDFs at these distances show well defined first coordination peaks at 3.7 Å. The appearance of these (Cl^-–CH_3) peaks indicates that the first solvation shell around the Cl^- ion are made up of DMSO molecules with their CH_3 groups oriented towards this ion. All these (Cl^-–O), (Cl^-–S), and (Cl^-–CH_3) RDFs show reduced intensities (in comparison to those near the Na^+ ion) indicating the diffuse nature of the solvation shell around the chloride ion. The fact that the ion–solvent RDFs do not change

beyond the SSIP distance of 7.2 Å has also been verified by computing the $g_{i\alpha}(r)$ functions at 10.0 Å and at 12.0 Å. The (Na^+–O), (Na^+–S), and (Na^+–CH_3) RDFs at these distances match exactly with those at 7.2 Å with respect to the peak positions and peak heights. The (Cl^-–O), (Cl^-–S), and (Cl^-–CH_3) RDFs at longer distances of 10.0 Å and 12.0 Å however differ marginally from those at 7.2 Å. That is, these larger distance RDFs show a slight increase (0.2 to 0.4 units) in the peak heights of (Cl^-–O) and (Cl^-–CH_3) RDFs, but the peak positions remain unchanged. Also, the (Cl^-–S) RDFs at those longer ion–ion distances show wider first peaks compared to that at 7.2 Å. The strongly bound coordination shell around the Na^+ ion is evidenced by the well defined and sharp ion–solvent RDF peaks appearing at 2.1 Å (for Na^+–O), 2.7 Å (for Na^+–S) and 4.2 Å (for Na^+–CH_3). Furthermore, the similarity between the RDF peaks at $r_{Na-Cl}=4.9$ Å (TS) and at $r_{Na-Cl}=7.2$ Å (SSIP) is in support of the Hammond postulate that the solvent configuration at the TS resembles more closely to that at the SSIP for the Na^+–Cl^- ion pair in DMSO. When the ions separate, the coordination shell around each ion also changes. This is analyzed by calculating the running coordination numbers,[31]

$$n_{i\alpha}(r)=4\pi\rho_\alpha\int_0^r g_{i\alpha}(s)s^2ds, \tag{7}$$

where ρ_α is the bulk number density of site α. These are displayed in Figs. 4 and 5, respectively, for the Na^+ ion and Cl^- ion, respectively. From Fig. 4, it can be seen that $n_{i\alpha}(r)$ for (Na^+–O) shows the formation of a strong coordination shell at a distance of 2.1 Å from the sodium end at all the three interionic distances studied. This is in conformity with the very intense peak (of intensity 28 units) seen in the RDF of this pair. The coordination shell for (Na^+–S) is not so strong at $r_{Na-Cl}=2.6$ Å, but its formation becomes complete when the interionic separation changes to $r_{Na-Cl}=4.9$ Å and $r_{Na-Cl}=7.2$ Å. For the (Na^+–CH_3) pair the coordination shell is not well defined, but nevertheless its presence can be seen by the near horizontal portions of the $n_{i\alpha}(r)$ curves at a distance of 4.7 Å from the sodium end. The reduced intensity of the $g_{i\alpha}(r)$ peak for this pair [Fig. 2(c)] causes its running coordination number to increase nearly continuously. Interestingly, the solvation shell around the Cl^- ion does not show a prominent shell structure as evidenced by the curves in Fig. 5, none of which shows any horizontal portions at any of the interionic distances studied. This is a bit surprising, given the fact that the (Cl^-–CH_3) RDF exhibits a sharp peak at 3.7 Å, although the peak intensity is less than 3 units. The (Cl^-–S) and (Cl^-–O) pairs also do not have horizontal portions in the $n_{i\alpha}(r)$ curves for the same reason.

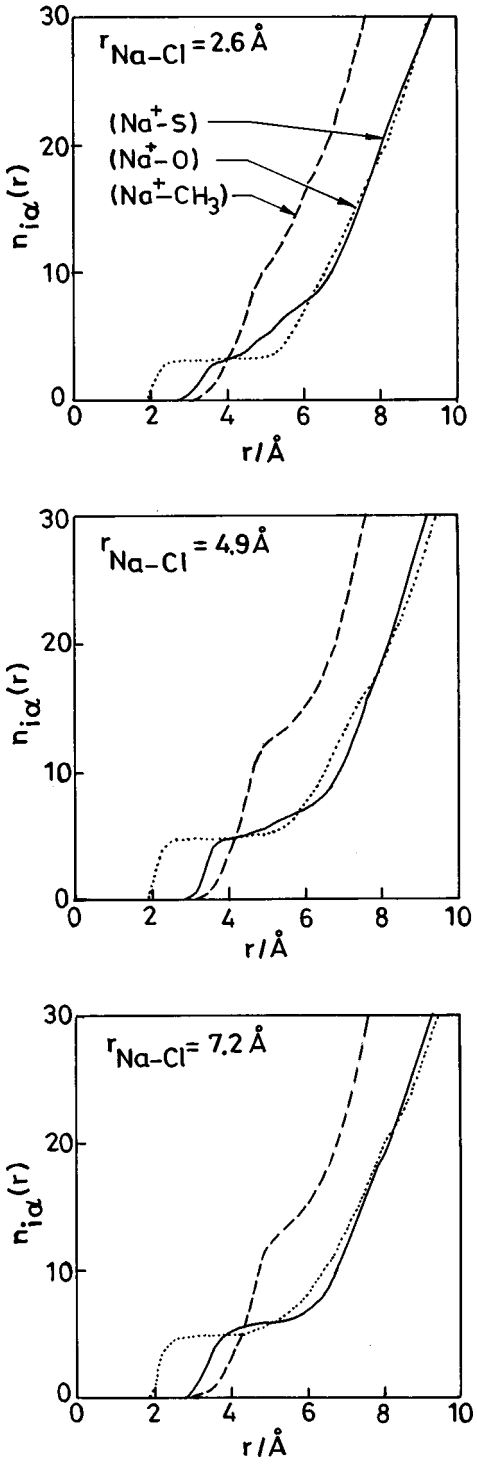

FIG. 4. The running coordination numbers of DMSO around the Na^+ ion at the three interionic separations.

IV. THE ORIENTATIONAL DISTRIBUTION FUNCTIONS

The angles (θ_i) and (ϕ_i) for each of the DMSO molecules were computed at each time step over a period of 50 ps for the five spatial regions (Fig. 1) defined earlier. We shall first discuss the distributions of the *bond inclination angles* θ_1 and θ_2 and then discuss the distributions of the *interplanar angles* (ϕ_i).

The $P(\theta_1)$ distributions in region 1 are shown in Fig. 6. For the three interionic distances of 2.6 Å, 4.9 Å, and 7.2 Å of the ion pair, the $P(\theta_1)$ functions in region 1 show a strong peak at $155°\pm2°$ with little variation in its position and intensity with change in ion–ion distances. We recall that the angle θ_1 is the inclination of the ($\overline{Na^+-S}$) and the ($\overline{S-O}$) bond vectors [Eq. (2a)]. The distributions of $P(\theta_1)$ functions in region 1 indicate a strong orientation of the polar sulphur–oxygen bond of the solvent towards the cation. Even though

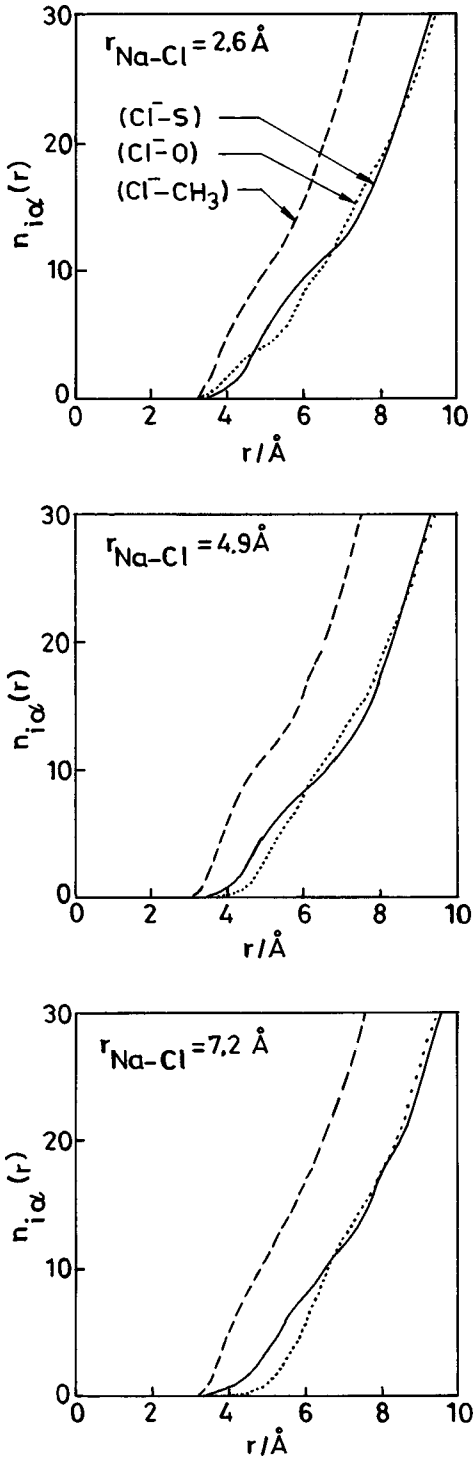

FIG. 5. The running coordination numbers of DMSO around the Cl^- ion at the three interionic separations.

the sulphur–oxygen bond vector is inclined to the molecular dipole vector at an angle of 21.2°, the corresponding $P(\theta_1')$ functions also show an intense peak around $150° \pm 5°$ (shown as an inset in Fig. 6). This implies that neither the bond vector nor the dipole vector are aligned directly towards the sodium ion. While no distance dependence is observed in the $P(\theta_1)$ functions, the corresponding functions $P(\theta_1')$ show a small distance dependence with respect to the positions of the peak maxima. That is, in region 1, the $P(\theta_1')$

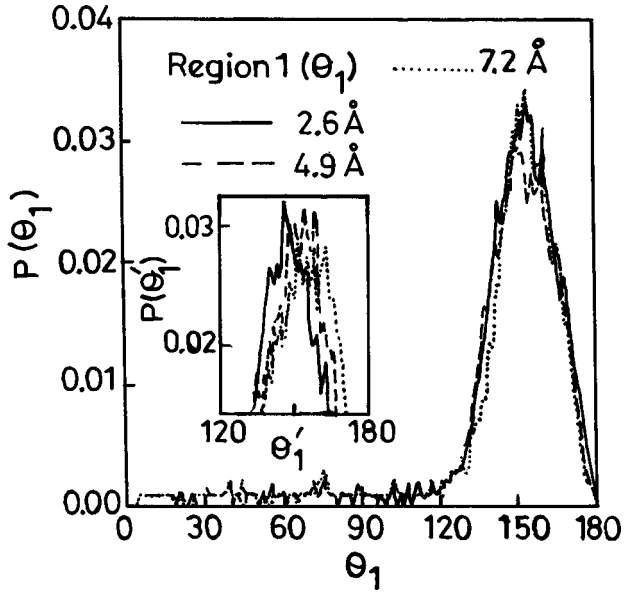

FIG. 6. Distribution of the $\theta_1 \equiv \cos^{-1}[(\overline{Na^+-S})\cdot(\overline{S-O})]$ angles in spatial region 1. The distribution of the $\theta_1' \equiv \cos^{-1}[(\overline{Na^+-COM})\cdot(\overline{COM-DIP})]$ angles which has some distance dependence in spatial region 1 is shown as an inset.

for $r_{Na-Cl} = 2.6$ Å shows the peak maximum at $148° \pm 2°$ and the $P(\theta_1')$ for $r_{Na-Cl} = 4.9$ Å and 7.2 Å show the peak maxima at $155° \pm 3°$. The intensity of the peak of the $P(\theta_1')$ distributions is about 10% smaller for the ion–ion distance of 7.2 Å in comparison with the other two distances.

The $P(\theta_2)$ distributions in region 4 are shown in Fig. 7. The angle θ_2 measures the inclination of the $(\overline{Cl^- - S})$ and the $(\overline{S-O})$ bond vectors [Eq. (2b)] and the angle θ_2' is the angle between the $(\overline{Cl^- - COM})$ and the $(\overline{COM-DIP})$ vectors. The corresponding distribution functions $P(\theta_2)$ and $P(\theta_2')$ exhibit a broad peak between 0° to 130° without any noticeable dependence on the interionic separation. This

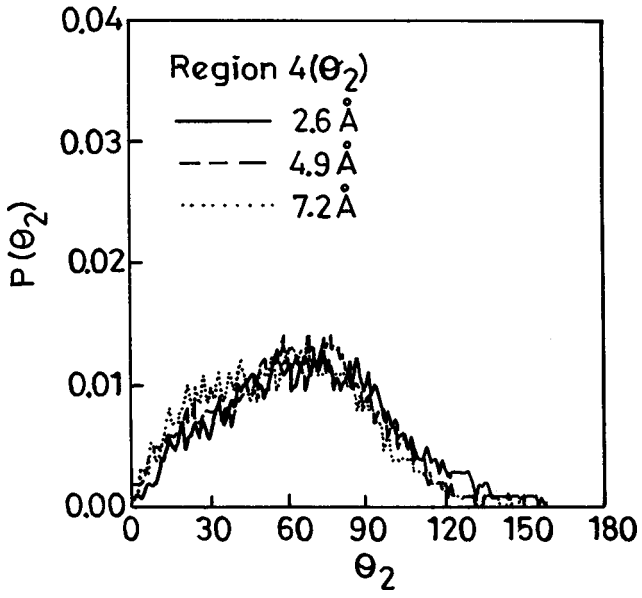

FIG. 7. Distribution of the $\theta_2 \equiv \cos^{-1}[(\overline{Cl^- - S})\cdot(\overline{S-O})]$ angles in spatial region 4.

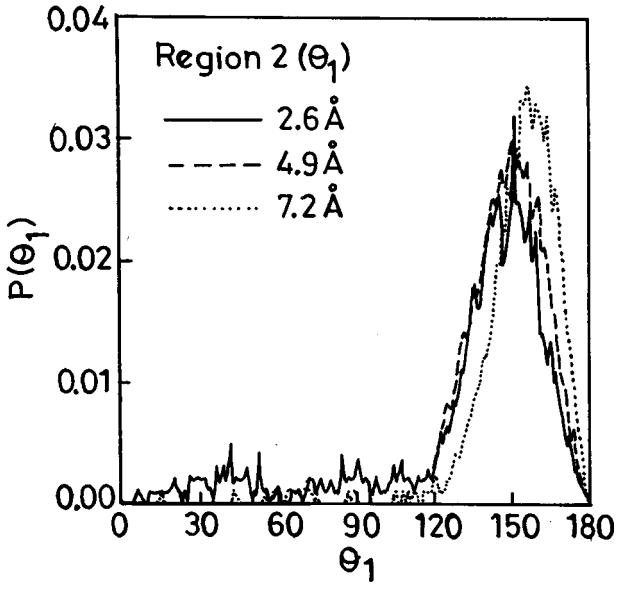

FIG. 8. Distribution of the $\theta_1 \equiv \cos^{-1}[(\overline{Na^+-S})\cdot(\overline{S-O})]$ angles in spatial region 2.

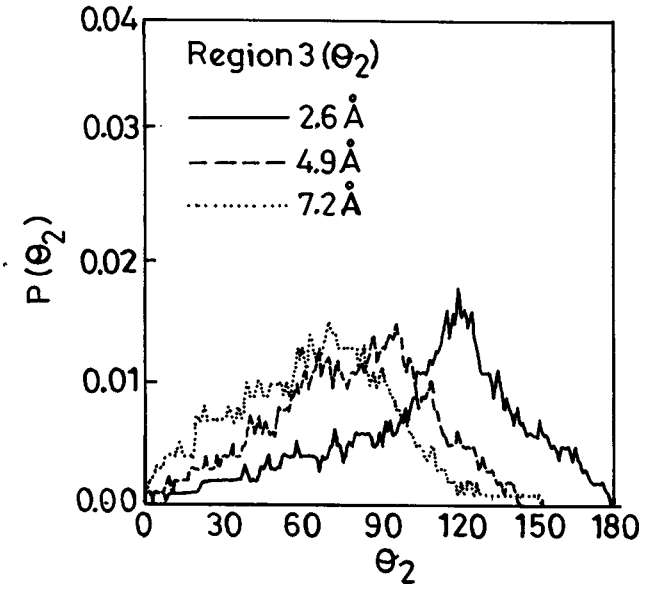

FIG. 9. Distribution of the $\theta_2 \equiv \cos^{-1}[(\overline{Cl^--S})\cdot(\overline{S-O})]$ angles in spatial region 3.

is attributed to the fact that the solvation shell for this ion is formed by the CH_3 groups of DMSO lying closer towards the ion and both the $(\overline{S-O})$ and $(\overline{COM-DIP})$ vectors are directed away from the $S-CH_3$ vectors. Hence the angles θ_2 and θ_2' will have wider variations depending on the nature of coordination of the Cl^- ion with only one CH_3 group of a DMSO molecule or with both the CH_3 groups of the same DMSO molecule, both of which are equally probable.

With respect to the dependence on interionic separation of the $P(\theta_i)$ functions, both region 2 and region 3 reveal interesting features. For the $P(\theta_1)$, the positions of the peak maxima in region 2 (Fig. 8) are at $148° \pm 2°$, $150° \pm 2°$, and $156° \pm 3°$ for $r_{Na-Cl} = 2.6$ Å, 4.9 Å, and 7.2 Å, respectively. With the increase in the ion–ion distance, the θ_1 angles change to larger magnitudes indicating stronger alignment of the $(\overline{S-O})$ and $(\overline{COM-DIP})$ vectors pointing towards the Na^+ ion, which gradually approaches near completion of its fully solvated single ion structure. We note here that the alignments of the $(\overline{S-O})$ bond vector and the $(\overline{COM-DIP})$ dipole vector towards the Na^+ ion show an almost identical trend as a function of the ion–ion distance. The spatial region left of the Cl^- ion (i.e., region 3) exhibits more prominent dependence of the $P(\theta_2)$ functions on the interionic separation. Here the peak maxima for the $P(\theta_2)$ function appear at $120° \pm 2°$, $98° \pm 2°$, and $66° \pm 3°$ for $r_{Na-Cl} = 2.6$ Å, 4.9 Å, and 7.2 Å, respectively (Fig. 9) for the orientation of the $(\overline{S-O})$ vector. The peaks at 4.9 Å and 7.2 Å are not sharp and appear in the range of 60°–110° (at $r_{Na-Cl} = 4.9$ Å) and 45°–90° (at $r_{Na-Cl} = 7.2$ Å). For the $(\overline{COM-DIP})$ orientation in this region the distribution function $P(\theta_2')$ exhibits similar peaks which are slightly sharper in appearance compared to the $(\overline{S-O})$ vector orientations. With the increase in ion–ion distance, the DMSO molecules in region 3 get better aligned with the CH_3 groups pointing towards the Cl^- ion, and the O atom pointing towards the Na^+ ion. This makes the angle θ_2 decrease with the increase in r_{Na-Cl}.

The fact that the solvent molecules in the bulk (i.e., in region 5) do not have a preferential orientation towards the ions with respect to either of the $(\overline{S-O})$ vector or the $(\overline{COM-DIP})$ vector is seen by the $P(\theta_i)$ distribution curves at $r_{Na-Cl} = 4.9$ Å in Fig. 10.

Let us now turn to the $P(\phi_i)$ functions for the orientation of the interplanar angles ϕ_i involving the Na^+-Cl^- ion pair and the different sites of the DMSO molecules. The unit vectors $(\hat{u}_i)$ are first computed from the respective $(\overline{ion-S})$

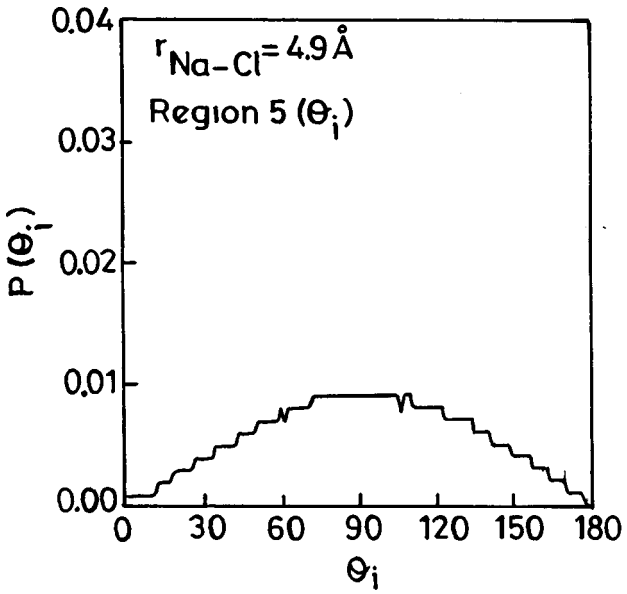

FIG. 10. The $P(\theta_i)$ distributions in the spatial region 5 at the interionic distance $r_{Na-Cl} = 4.9$ Å. For the other two distances of 2.6 Å and 7.2 Å, the distributions are almost identical. The $P(\theta_1)$, $P(\theta_1')$, $P(\theta_2)$, and $P(\theta_2')$ distributions in this region are almost identical for all the three ion–ion separations and θ_i in the figure refers to any of these four angles.

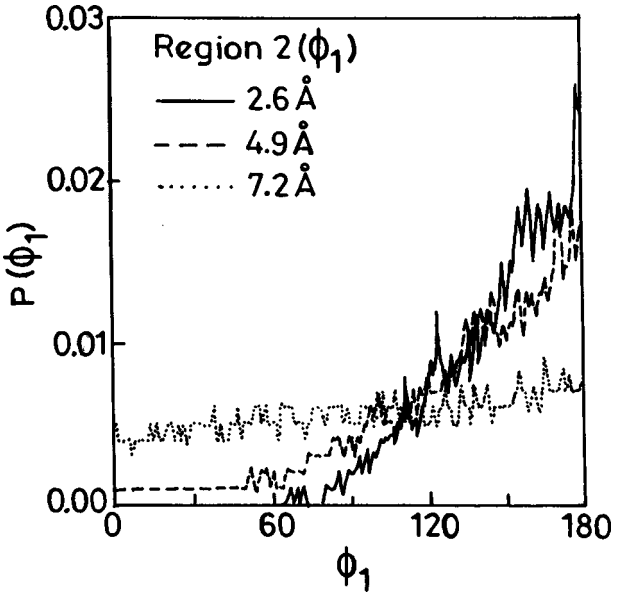

FIG. 11. Distribution of the interplanar angle ϕ_1 [angle between the plane containing (S, Na^+, and Cl^-) and the plane containing (Na^+, S, and O)] in spatial region 2.

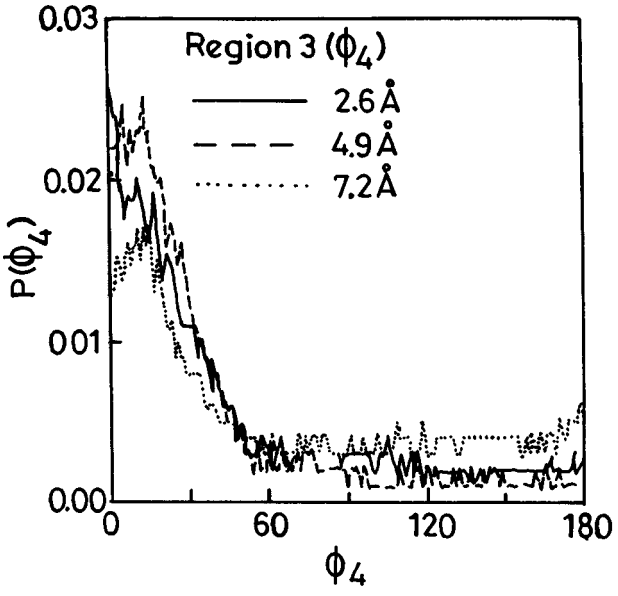

FIG. 13. Distribution of the interplanar angle ϕ_4 [angle between the plane containing (S, Cl^-, and Na^+) and the plane containing (Cl^-, S, and O)] in spatial region 3.

vectors. These are then projected into the plane containing the Na^+ ion, the Cl^- ion and the S atom of DMSO. Finally the angles ϕ_i are computed. The $P(\phi_i)$ distributions in regions 2 and 3 are displayed in Figs. 11–14.

In region 1, the magnitudes of $P(\phi_1)$ as well as $P(\phi_2)$ distributions are limited within 0.002 to 0.010. Likewise, in region 4, the magnitudes of $P(\phi_4)$ and the $P(\phi_5)$ distributions are limited within 0.002 and 0.008. There is no significant distance dependence in these distributions.

Both the regions 2 and 3 exhibit significant variations in the $P(\phi_1)$, $P(\phi_2)$, $P(\phi_4)$, and $P(\phi_5)$ distributions with interionic separations. The $P(\phi_1)$ distributions in region 2 are shown in Fig. 11. The angle ϕ_1 [defined in Sec. II, Eqs. (3) and (4)] can vary between 0° and 180°. At short distances of $r_{Na-Cl}=2.6$ Å and 4.9 Å, the $P(\phi_1)$ distributions show preference to larger angles (>90°). The $P(\phi_1)$ distributions at large r_{Na-Cl} are nearly flat (magnitude 0.004) with almost equal population for all the ϕ_1 angles. The preference towards larger angles at $r_{Na-Cl}=2.6$ Å and 4.9 Å is because the unit vectors $\hat{u}_1$ and $\hat{u}_2$ (centered at S and Na sites, respectively) are aligned away from each other at these ion–ion distances. Because of the proximity of the Cl^- ion in this region, the S of DMSO can come closer (within 3.2 Å) to the Na^+ ion. At the longer interionic separation of 7.2 Å the

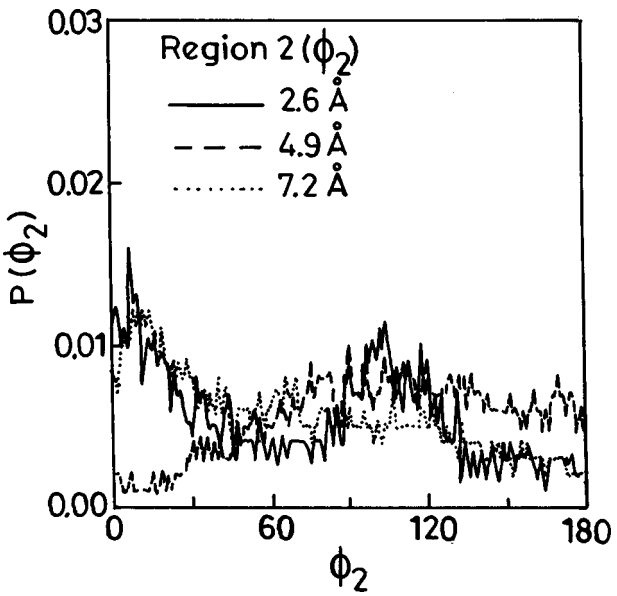

FIG. 12. Distribution of the interplanar angle ϕ_2 [angle between the plane containing (S, Na^+, and Cl^-) and the plane containing (Na^+, S, and CH_3^{mid})] in spatial region 2.

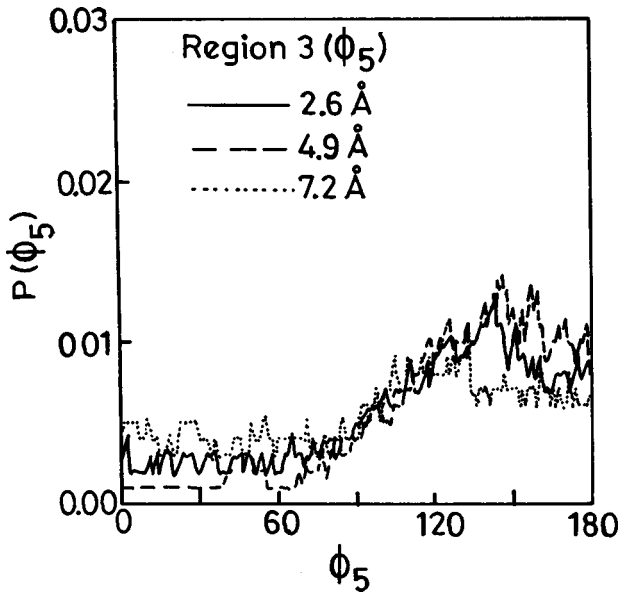

FIG. 14. Distribution of the interplanar angle ϕ_5 [angle between the plane containing (S, Cl^-, and Na^+) and the plane containing (Cl^-, S, and CH_3^{mid})] in spatial region 3.

influence of the Cl^- ion gets reduced; also the Na^+ ion tends to form its own coordination shell with the O atoms of DMSO pointing towards it. As a consequence, the angle of inclination between the unit vectors $\hat{u}_1$ and $\hat{u}_2$ can vary from 0° and 180° making the $P(\phi_1)$ distribution nearly flat at $r_{Na-Cl}=7.2$ Å. The $P(\phi_2)$ distributions in region 2 are limited between 0.001 and 0.015 with an average intensity of 0.005 (Fig. 12). The angle ϕ_2 gauges the relative alignments of the plane containing (S atom, Na^+ ion, and Cl^- ion) with the plane containing (Na^+ ion, S atom, and CH_3^{mid}). Here, the short distance ($r_{Na-Cl}=2.6$ Å) $P(\phi_2)$ distribution is slightly different from those at longer ion-ion distances ($r_{Na-Cl}=4.9$ Å and 7.2 Å). The reasons for such behavior in the $P(\phi_2)$ distributions in this region are as follows. Since the two CH_3 groups of DMSO are directed towards the Cl^- ion, the relative alignment of the $(\overline{S-CH_3^{mid}})$ vector with the interionic vector in region 2 shows a preference to smaller angles at the larger interionic separations of 4.9 Å and 7.2 Å. However, the $P(\phi_2)$ distribution of such a preference is restricted only up to 0.012.

The $P(\phi_4)$ distributions in region 3 also exhibit distinct dependence on the interionic separations (Fig. 13). The distributions are significantly intense with preferred angles less than 60° for all the interionic distances of $r_{Na-Cl}=2.6$ Å, 4.9 Å and 7.2 Å. The preference to the smaller angles can be understood as follows. The angle ϕ_4 relates to the relative inclination of the plane containing (Cl^- ion, S atom and O atom) with the plane containing (S atom, Cl^- ion, and Na^+ ion). In region 3, the O atoms of DMSO molecules are directed towards the Na^+ ion, making the relative alignments of the $(\overline{S-O})$ and $(\overline{Cl^- - Na^+})$ vectors almost parallel. This makes the angle ϕ_4 smaller. The distance dependence of the $P(\phi_4)$ distributions shows gradual reduction of intensities as one increases the ion–ion distance from 2.6 Å to 4.9 Å to 7.2 Å. The relative near parallel alignments of these $(\overline{S-O})$ and $(\overline{Cl^- - Na^+})$ vectors get perturbed as the Na^+ ion is moved away. The magnitudes of $P(\phi_5)$ distributions in this region 3 are limited between 0.001 to 0.013, and the distance dependence is just opposite to those seen for $P(\phi_4)$ distributions in this region, albeit with reduced intensities (Fig. 14). The angle ϕ_5 measures the relative alignment of the plane containing (S atom, Cl^- ion, and Na^+ ion) with the plane containing (Cl^- ion, S atom, and CH_3^{mid}). The preference of the angles ϕ_5 to larger values is due to the approach of the CH_3 groups towards the Cl^- ion in order to form the first coordination shell around this ion. As a consequence, the $(\overline{Cl^- - CH_3^{mid}})$ and $(\overline{Cl^- - Na^+})$ vectors tend to get aligned at angles more than 90°. The dependence on interionic separation for the $P(\phi_5)$ distributions in this region 3 is not very significant. The $r_{Na-Cl}=2.6$ Å and 4.9 Å distributions are nearly identical but the distribution corresponding to the $r_{Na-Cl}=7.2$ Å is marginally different showing reduced preference of the ϕ_5 angles to larger ($>90°$) values.

In region 5, all of the $P(\phi_1)$, $P(\phi_2)$, $P(\phi_4)$, and $P(\phi_5)$ distributions show an average intensity of 0.005 units (not shown), and these distributions do not show any observable dependence on r_{Na-Cl}. The angles ϕ_3 and ϕ_6 correspond to the intramolecular angles between $(\overline{S-O})$ and $(\overline{S-CH_3^{mid}})$ vectors. Hence the $P(\phi_3)$ and $P(\phi_6)$ distributions corresponding to these angles show an intense peak maximum at 117.1° (this is the angle between the $(\overline{S-O})$ bond vector and the $(\overline{S-CH_3^{mid}})$ bond vector in a DMSO molecule) irrespective of the region in which the solvent molecule resides. The $P(\phi_3)$ and $P(\phi_6)$ distributions are of the intramolecular angles only and hence have not been shown.

V. CONCLUSIONS

The solvation of the Na^+Cl^- ion pair in DMSO has been examined in terms of the ion-solvent radial distribution functions and the ion–solvent orientational distribution functions. The solvation shell at the sodium ion end is composed of three DMSO molecules at the CIP configuration and contains five DMSO molecules at the TS and at the SSIP configurations. The chloride end of the ion pair has a somewhat diffuse solvation shell with the methyl groups of the DMSO molecules staying closer to this ion. At the CIP configuration, the chloride end of the ion pair shows the Cl^-–O coordination shell to be the closest, in which the oxygen atom is actually from the Na^+–O shell due to the proximity of the Na^+ ion. At the TS and SSIP configurations, the chloride end solvation shell is formed by the CH_3 groups of DMSO at a distance of 3.7 Å.

In order to have a complete understanding of the solvation process during CIP⇔SSIP interconversion, the results on the radial distributions of the solvent molecules are required to be supplemented by the orientational distributions. Our results on the three states of the Na^+Cl^- ion pair in DMSO, viz., the CIP, the TS and the SSIP, indicate a strong orientational dependence of the reactant solvation shell, especially at the sodium end during its passage from the CIP to the TS to the SSIP. The $(\overline{Na^+ - S})$ and the $(\overline{S-O})$ vectors (the horizontal superscript line on the connecting ions/atoms indicates the vector from the first site to the second site) are inclined to each other at an angle $155° \pm 2°$. The $(\overline{Na^+ - COM})$ and the $(\overline{COM - DIP})$ vectors (COM is the center of mass of the DMSO molecule and DIP is the tip of the dipole moment vector) are also inclined to each other with an angle of similar magnitude at the sodium end. The peaks in the dipole orientation functions $P(\theta_i')$ show a small dependence on the interionic distance even in region 1. These results at the sodium end differ from the orientations of water molecules in the solvation shell of Na^+ ion in water where the corresponding angle is seen to be close to 180°.[16]

It is also interesting to note that in the studies of the liquid membrane structures, the tilt of the hydrocarbon chains with respect to the bilayer normal (0° pointing from the hydrocarbon to water, normal to the bilayer plane) is also around 150°. The sharpness of all the peaks referred to above are very similar.[18] In the case of the lipid membrane simulations, it is found that many experimental observables such as the order parameters are reproduced in the simulations. The experiments to study the distance dependence of the orientational distributions around the ion pair are much more difficult to perform.

The orientational dependences of $[P(\theta_2)]$ and $[P(\theta_2')]$ in the solvation shell at the chloride end are not as sharply

peaked as the ones near the sodium end. The inclinations of the ($\overline{Cl^-–S}$) and the ($\overline{S–O}$) vectors (represented as angle θ_2) are in the range of 20°–100° around the chloride ion in region 4. Similarly the inclinations of the ($\overline{Cl^-–COM}$) vector with the ($\overline{COM–DIP}$) vector (represented as angle θ_2') also show an identical distribution in this region. In the spatial region 3 we observe the largest distance dependence in $P(\theta_2)$ and $P(\theta_2')$. At 2.6 Å, both these distributions are peaked at 120° and as the distance increases to 7.2 Å these distributions become similar to those in region 4.

The distance dependence of the distributions of the interplanar angles (in which one of the planes contain the Na^+ ion, the Cl^+ ion, and the S atom) are not very pronounced. We have not observed any significant preferential alignments of the $Na^+–S–O$ plane or the $Na^+–S–CH_3^{mid}$ plane with respect to the $S–Na^+–Cl^-$ plane. Similarly the $Na^+–COM–DIP$ plane or the $Na^+–COM–CH_3^{mid}$ plane do not show any preferred alignment with respect to the $COM–Na^+–Cl^-$ plane. Identical observations are made at the chloride end of the ion pair. These broad distributions are indicative of a very weak second solvation shell around the ion pair in DMSO. In contrast, the second solvation shell for the same $Na^+–Cl^-$ ion pair is very prominent in water because of the extensive tetrahedral network of hydrogen bonds.[16] Thus the very weak second solvation shell for the $Na^+–Cl^-$ in DMSO gives another evidence of the near absence of hydrogen bonding in DMSO.

It will be of interest to extend this study of orientational distributions to include all the Euler angles representing each solvent molecule.[17] Such a study, especially of the ion pair in water will provide another structural representation of hydrogen bonding in the vicinity of the ion pairs and will also aid in the calculation of the entropy changes accompanying solvation. The details of the mechanism of stripping of water molecules and ions from a protein surface[22] may also be understood better through the orientational distribution functions. While the angles θ_1' (the angle between the Na^+ ion–COM vector and the dipole vector originating at the COM) are nearly 180° for water around the Na^+ ion, for DMSO these angles are 155°. Towards the Cl^- ion, the corresponding ranges for angles θ_2' are 30°–60° in water (quite sharply peaked) and 20°–100° in DMSO. It would be of great interest to see the variations of these angular distributions in other solvents.

[1] (a) P. W. Atkins, *Physical Chemistry*, 5th ed. (Oxford University Press, Oxford, 1995); (b) N. S. Isaacs, *Physical Organic Chemistry*, 1st ed. (English Language Book Society/Longman, Essex, 1990).
[2] A. J. Orr-Ewing and R. N. Zare, Annu. Rev. Phys. Chem. **45**, 315 (1994).
[3] *Ions and Ion Pairs and their Role in Chemical Reactions*, edited by J. Smid (Pergamon, Oxford, 1979).
[4] *Ions and Ion Pairs in Organic Reactions*, edited by M. Szwarc (Wiley, New York, 1972), Vol. 1.
[5] *Ions and Ion Pairs in Organic Reactions*, edited by M. Szwarc (Wiley, New York, 1974), Vol. 2.
[6] J. E. Gordon, *The Organic Chemistry of Electrolyte Solutions* (Wiley, New York, 1975).
[7] G. Ciccotti, M. Ferrario, J. T. Hynes, and M. Kapral, J. Chem. Phys. **93**, 7137 (1990).
[8] O. A. Karim and J. A. McCammon, Chem. Phys. Lett. **132**, 219 (1986).
[9] R. Rey and E. Guardia, J. Phys. Chem. **96**, 4712 (1992).
[10] G. Sese, E. Guardia, and J. A. Padro, J. Phys. Chem. **99**, 12647 (1995).
[11] A. K. Das, M. Madhusoodanan, and B. L. Tembe, J. Phys. Chem. A **101**, 2862 (1997).
[12] H. A. Kramers, Physica (Amsterdam) **7**, 284 (1940).
[13] R. F. Grote and J. T. Hynes, J. Chem. Phys. **73**, 2715 (1980).
[14] D. J. Raber, J. M. Harris, and P. R. Schleyer, in *Ions and Ion Pairs in Organic Reactions*, edited by M. Szwarc (Wiley, New York, 1974), Vol. 2.
[15] G. van der Szwan and J. T. Hynes, J. Chem. Phys. **76**, 2993 (1982).
[16] A. C. Belch, M. Berkowitz, and J. A. McCammon, J. Am. Chem. Soc. **108**, 1765 (1986).
[17] T. Lazaridis, and M. Karplus, J. Chem. Phys. **105**, 4294 (1996).
[18] T. R. Stouch, Mol. Simul. **10**, 335 (1993).
[19] R. Brasseur, M. Vandenbranden, A. Burny, and J. M. Ruysschaert, in *Molecular Description of Biological Membranes by Computer Aided Conformational Analysis*, edited by R. Brasseur (Chemical Rubber, Boston, 1990), Vol. II.
[20] D. A. Binder and M. M. Kreevoy, J. Phys. Chem. A **101**, 1774 (l997).
[21] B. R. Arnold, S. Farid, J. L. Goodman, and I. R. Gould, J. Am. Chem. Soc. **118**, 5482 (1996).
[22] Ya-Jun Zheng and R. L. Ornstein, J. Am. Chem. Soc. **118**, 4175 (1996).
[23] T. J. Anchordoguy, C. A. Ceccini, J. N. Crowe, and L. M. Crowe, Cryobiology **28**, 467 (1991).
[24] S. W. Jacob and R. Herschler, Cryobiology **23**, 14 (1986).
[25] A. P. Krapcho, Synthesis 805 (1982); 893 (1982).
[26] M. Madhusoodanan and B. L. Tembe, J. Phys. Chem. **98**, 7090 (1994).
[27] M. Madhusoodanan and B. L. Tembe, J. Phys. Chem. **99**, 44 (1995).
[28] J. P. Hansen and I. R. McDonald, *Theory of Simple Liquids* (Academic, San Diego, 1990).
[29] L. Verlet, Phys. Rev. **159**, 98 (1967).
[30] J. P. Ryckaert, G. Ciccotti, and H. J. C. Berendsen, J. Comput. Phys. **23**, 927 (1977).
[31] I. I. Vaisman and M. L. Berkowitz, J. Am. Chem. Soc. **114**, 7889 (1992).